








Development of ventricular trabeculae affects electrical conduction in the early endothermic heart

Veronika Olejnickova^{1,2}  | Peter Uriel Hamor¹ | Jiri Janacek³  |
 Martin Bartos^{1,4}  | Eva Zabrodska¹ | Barbora Sankova¹  |
 Alena Kvasilova¹  | Hana Kolesova^{1,2}  | David Sedmera^{1,2} 

¹Institute of Anatomy, First Faculty of Medicine, Charles University, Prague, Czech Republic

²Laboratory of Developmental Cardiology, Institute of Physiology, Czech Academy of Sciences, Prague, Czech Republic

³Laboratory of Biomathematics, Institute of Physiology, Czech Academy of Sciences, Prague, Czech Republic

⁴Department of Stomatology, General University Hospital in Prague, First Faculty of Medicine, Charles University, Prague, Czech Republic

Correspondence

Veronika Olejnickova, Charles University, First Faculty of Medicine, Institute of Anatomy, U Nemocnice 3, 12800 Prague 2, Czech Republic.

Email: veronika.olejnickova@lf1.cuni.cz

Funding information

Czech Health Research Council, Grant/Award Number: NU21J-02-00039; Czech Science Foundation, Grant/Award Number: 22-05271S; National Institute for Research of Metabolic and Cardiovascular Diseases (Programme EXCELES, ID Project No. LX22NPO5104) - Funded by the European Union - Next Generation EU.

Abstract

Background: The ventricular trabeculae play a role, among others, in the impulse spreading in ectothermic hearts. Despite the morphological similarity with the early developing hearts of endotherms, this trabecular function in mammalian and avian embryos was poorly addressed.

Results: We simulated impulse propagation inside the looping ventricle and revealed delayed apical activation in the heart with inhibited trabecular growth. This finding was corroborated by direct imaging of the endocardial surface showing early activation within the trabeculae implying preferential spreading of depolarization along with them. Targeting two crucial pathways of trabecular formation (Neuregulin/ErbB and Nkx2.5), we showed that trabecular development is also essential for proper conduction patterning. Persistence of the slow isotropic conduction likely contributed to the pumping failure in the trabeculae-deficient hearts.

Conclusions: Our results showed the essential role of trabeculae in intraventricular impulse spreading and conduction patterning in the early endothermic heart. Lack of trabeculae leads to the failure of conduction parameters differentiation resulting in primitive ventricular activation with consequent impact on the cardiac pumping function.

KEYWORDS

embryonic chick heart, neuregulin/ErbB, Nkx2.5, ventricular trabeculae

1 | INTRODUCTION

The heart is essential for embryonic survival and one of the first functioning organs during embryogenesis. Its periodic contractions appear shortly after its formation to drive circulation and allow embryonic growth.¹ The

cardiac movement is driven by a pacemaker positioned at the inflow region in birds² and mammals.³ First, the contraction is determined by the isotropic fashion of conduction.^{3,4} This slow movement progresses along the heart tube in a peristaltoid isotropic manner.⁵ Subsequently, the conduction pattern is diversified according to the

This is an open access article under the terms of the [Creative Commons Attribution](https://creativecommons.org/licenses/by/4.0/) License, which permits use, distribution and reproduction in any medium, provided the original work is properly cited.

© 2022 The Authors. *Developmental Dynamics* published by Wiley Periodicals LLC on behalf of American Association for Anatomy.

particular heart segment.^{6,7} The conduction becomes anisotropic in the looping ventricle, ensuring fast and coordinated chamber activation. The primary interventricular ring (PIR) as an intermediate state is rapidly replaced by the apex-first (with right and/or left epicardial breakthrough) activation sequence. These advanced patterns appeared from embryonic day (ED) ED9.5 in mice and ED4 in chicks.^{6,8-10} In the same period, the developing trabecular network coarsens luminal the surface of the ventricle.¹¹ In addition to their other functions, at least in part of ectotherms, trabeculae play a role in interconnecting the atrioventricular canal (AVC) to the ventricular apex, thus, providing a shortcut for activation wave. In the amphibians (namely *Xenopus laevis*) and fish (namely zebrafish and African lungfish), the apex-first activation pattern was observed and associated with the trabecular system.^{12,13} Despite the superficial morphological similarities between ectothermic and embryonal endothermic hearts, whether the trabecular design of early endothermic ventricles plays a similar role in the electrical conduction has not been directly addressed yet. This study analyzed intraventricular conduction by either simulation of impulse propagation or direct measurement of opened ED4 chick ventricle using high-speed optical imaging. In addition, we created a novel trabeculae-deficient chick model by pharmacologically targeting Neuregulin/ErBb pathway. This model, together with the mouse *Nkx2.5*^{-/-} heart, allowed us to investigate conduction patterns of trabeculae-deficient heart in both prototypic endothermic animals. We showed that trabeculae development allows faster electrical wave propagation and earlier apex activation. Both trabeculae-deficient models showed an isotropic activation pattern without progression to the more advanced anisotropic activation sequence. Moreover, the level of trabeculation was shown to be negatively correlated with the ventricular activation time, highlighting the role of trabeculation in the initiation of faster anisotropic ventricular conduction.

2 | RESULTS

2.1 | The developing trabeculae allow earlier apex activation

To investigate the role of ventricular trabeculae in impulse spreading during early cardiac development of endotherms, we simulated impulse propagation in the three-dimensional (3D) reconstructed datasets of the trabeculae-deficient (induced by AG1478 treatment—an inhibitor of the ErbB1 receptor and the ErbB2/ ErbB3 heterodimer) and control looping chick heart at the

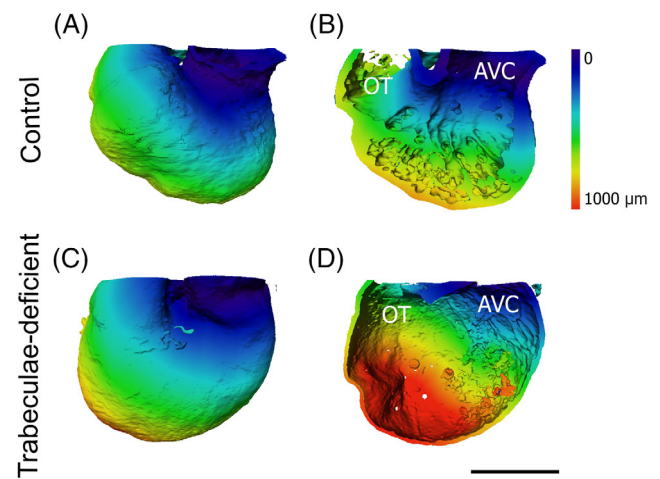


FIGURE 1 Simulated activation of ventricular apex shows earlier apex activation chick trabeculated heart. The surface view of the simulation shows a delayed apex activation in the reconstructed chick trabeculae-deficient (A) compared with the control ventricle (C). Panels B and D show intraventricular views of the simulations. Whereas in the trabeculae-deficient heart, the impulse is spread on the ventricular wall only (B), activation is spread along the trabeculae providing the shortcut to apex activation in the control hearts (D). $n = 3$ for both trabeculae-deficient and control hearts. A, atrium; OT, outflow tract; Tr, ventricular trabeculae. Scale bar 500 μm

Hamburger-Hamilton (HH)¹⁴ stage 19. We used a model based on geodesic distance adapted to the embryonic heart.^{15,16} When the impulse was initiated at the AVC perimeter where the atrioventricular conduction is present, delayed apex activation in the trabeculae-deficient chamber (Figure 1C) compared to controls (Figure 1A) was observed. The internal view (Figure 1B, D) showed a difference in the intraventricular conduction by the trabecular system or the ventricular wall only. The delayed apex activation was observed in all analyzed trabeculae-deficient hearts.

We further approached the intraventricular conduction directly by imaging the endocardial aspect of the chick-looping heart (HH24; Figure 2). In this embryonic stage, the trabeculae are well developed but still not compacting,^{17,18} enabling visualization of impulse propagation through the trabecular network. Using optical mapping, we observed that the first depolarization appeared in the atrioventricular area and the inner area of the ventral part of the ventricle (Figure 2A). This area corresponded with the presence of trabeculae in the mapped heart (Figure 2B). The depolarization wave subsequently propagated to the adjacent cardiac tissue to reach the ventricular apex (this activation pattern was observed in all analyzed hearts). When optical mapping was performed from the epicardial surface of the same

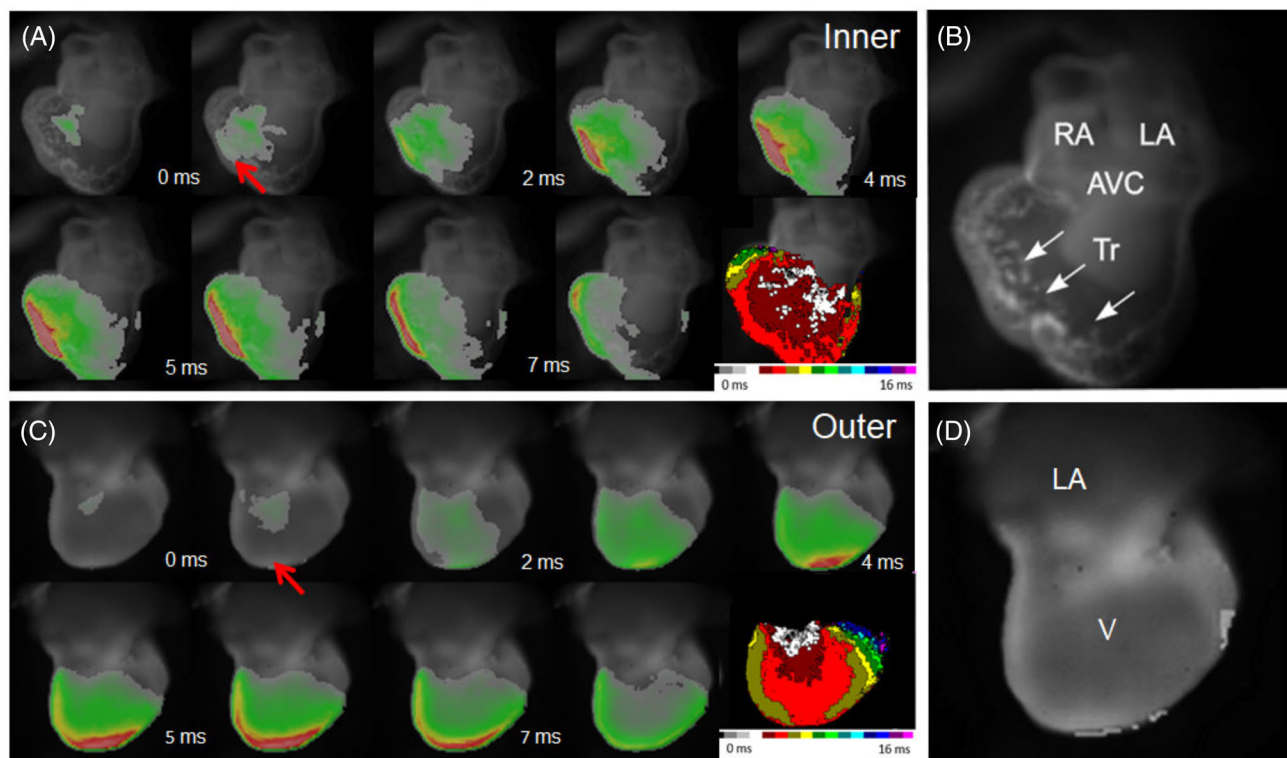


FIGURE 2 Ventricular trabeculae are the first activated area within the intraventricular surface. Representative image of activation wave propagation at the endocardial (A) and epicardial (C) aspect of HH24 chick heart ($n = 5$). The early activated area corresponds to the developing trabeculae in the intracardiac view (A, red arrow) and later activation of the same area in the epicardial view (C, red arrow). Grayscale images of the analyzed area are shown on panels B and D. AVC, atrioventricular canal; LA, left atrium; RA, right atrium; Tr, ventricular trabeculae

heart (before cutting, either anterior or posterior view; Figure 2D), the ventricular apex was activated later than in optical mapping performed from the intraventricular aspect (4.2 ± 0.4 ms from the outer aspect vs 3.4 ± 0.5 ms from inner aspect; Figure 2). In the epicardial maps, the nonconcentric shape of the isochrones directed to the apex was observed. This corresponded well with the prevailing trabecular orientation at this stage (Figure 2B^{10,17}) as well as with the prediction of the simulation model (Figure 1).

2.2 | Trabeculae-deficient models show thin ventricular walls and insufficient cardiac function

To confirm the role of the early ventricular trabeculae in conduction, we analyzed the activation patterns in ventricles without trabeculae. First, we adapted the previously described trabeculae-deficient model created by targeting Neuregulin/ErbB signaling for the endothermic heart. The AG1478 was applied adjacent to the developing heart before trabecular emergence. The mortality of treated

embryos was 37% (18/49). Disruption of the Neuregulin/ErbB pathway resulted in a severe deficit in trabeculation (Figure 3C), albeit only in a narrow window of its application (Table S1). This window coincided well with the period of early trabecular emergence in the chick.^{17,18} The optimum time frame for a successful trabecular inhibition by AG1478 was around 62 hours of incubation when the ventricle started the ballooning process. The earlier application could not block the signaling pathway, and during the later inhibition, the trabecular process was already established and thus no longer sensitive to inhibition (Table S1).

Both control and AG1478-treated hearts possessed tubular morphology in HH stage 17 (Figure 4A). While control hearts continued in normal development with trabeculae appearing first in the outer curvature of the ventricle and filling up a substantial part of the ventricle at HH18-19 (Figures 3A and 4A), we observed heart dilatation and a thin ventricular wall at HH18-19 in 14 out of 22 AG1478-treated embryos at HH18-19 (Figures 3C and 4C). Development of the trabeculae-deficient phenotype was accompanied with decreased heart rate. While in controls, heart rate continued to significantly rise (from

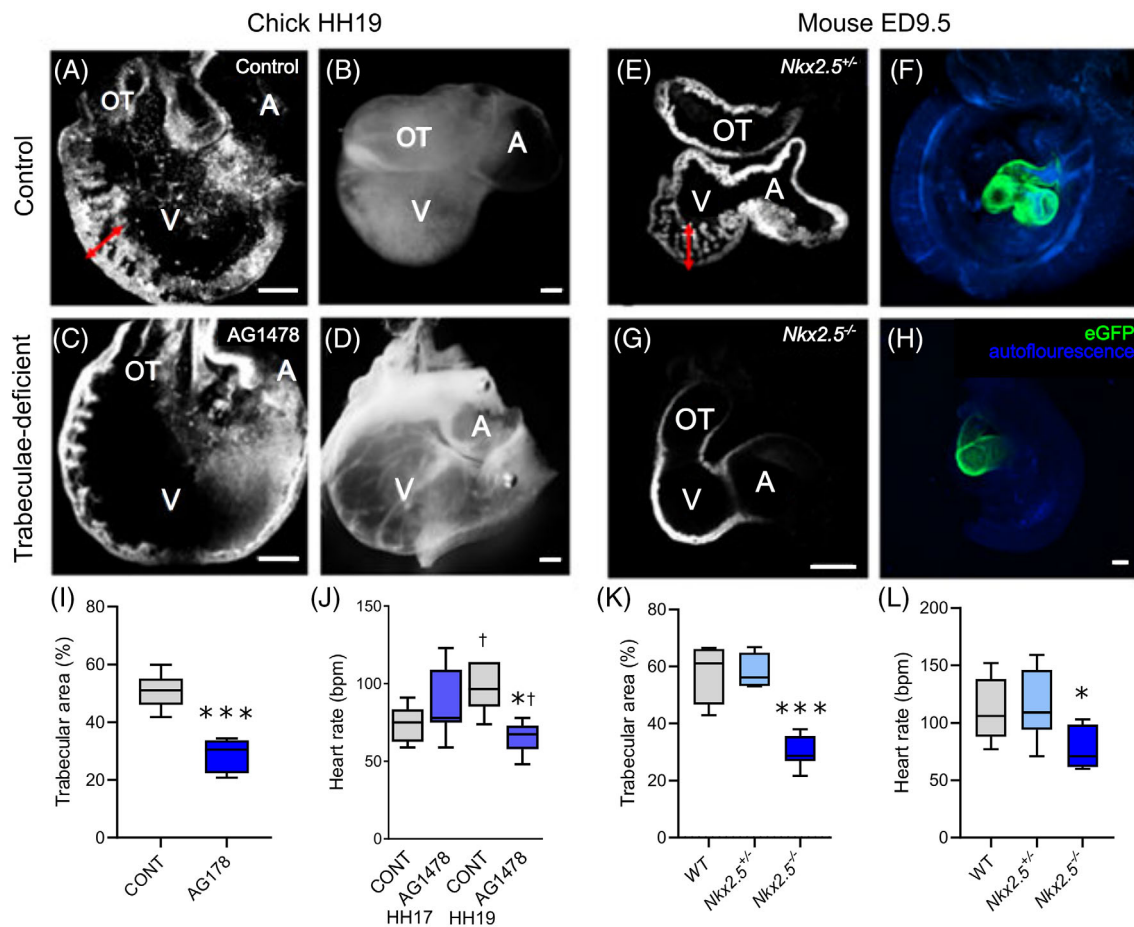


FIGURE 3 Trabeculae-deficient models possess a smooth and thin ventricular wall and altered function. Representative section of a control chick (A) and mouse (E) hearts showing extensive trabeculation of the ventricular wall at the looping stage (red double-headed arrows). Surface view of these hearts depicting the standard dimensions of the looping chick (B) and mouse (F) hearts. In contrast, optical sections of trabeculae-deficient hearts show a dramatic reduction in the trabeculation resulting in relative ventricular wall thinning in both chick (C) and mouse (G) models resulting in the ventricular dilatation of the AG1478 chick hearts (D) and smooth ventricular wall without any trabeculae in the *Nkx2.5*^{-/-} mouse (H). The level of trabecular layer was significantly reduced in both trabeculae-induced models (*t*-test; $n = 6$ animals per group in chick, I; one-way ANOVA and subsequent Student-Newman-Keuls test, $n = 4-7$ per group in mouse, K). The analysis of heart rate showed a significant decrease in both HH19 chick (*t*-test, $n = 6$ per group, J) and *Nkx2.5*^{-/-} mice (one-way ANOVA and subsequent Student-Newman-Keuls test; $n = 10-14$ animals per group, L). A, atrium; V, ventricle; OT, outflow tract. Scale bar 200 μm . All data are expressed as means \pm SD; in mouse: *** $P < .0001$ vs WT and *Nkx2.5*^{+/-}; in chick: * $P < .05$ vs control HH19, † $P < .05$ vs corresponding HH17 stage, *** $P < .0001$ vs control HH19

74 ± 12 bpm to 97 ± 16 bpm in HH17 and HH18-19, respectively; $P < 0.05$), a drop ($P = 0.073$) in beating frequency was observed in the treated group (from 89 ± 23 bpm to 65 ± 10 bpm in HH17 and HH18-19, respectively; Figure 3J). AG1478-treated hearts also showed irregular beating (not observed in controls), distended ventricles and compromised function with decreased contractility (Figure 4C, Supplementary Movie S1 and S2). This phenotype resulted in embryonic mortality past the stage HH19.

The *Nkx2.5*^{GFP} knock-in mouse was used as a second model of the trabeculae-deficient heart. We also analyzed ErbB2-mutated mouse line, but we preferred *Nkx2.5*^{GFP}

knock-in mice due to the more pronounced phenotype. The heterozygous state (denoted as *Nkx2.5*^{+/-}) presented heart morphology and survival rate similar to wild-type (WT) embryos as we described recently.¹⁶ In the ED9.5 homozygote *Nkx2.5*^{GFP/GFP} embryos (denoted as *Nkx2.5*^{-/-}), we observed tube-shaped morphology resembling the earlier tubular heart (Figure 3H). In contrast to the WT and *Nkx2.5*^{+/-} (Figure 3E, F), the inner surface of the *Nkx2.5*^{-/-} ventricle was smooth with a complete lack of trabecular development (Figure 3G). A significantly decreased crown-rump length (CRL) was observed in the *Nkx2.5*^{-/-} compared with both *Nkx2.5*^{+/-} and WT (2.9 ± 0.5 , 4.2 ± 1.3 , and 4.5 ± 0.6 mm for *Nkx2.5*^{-/-},

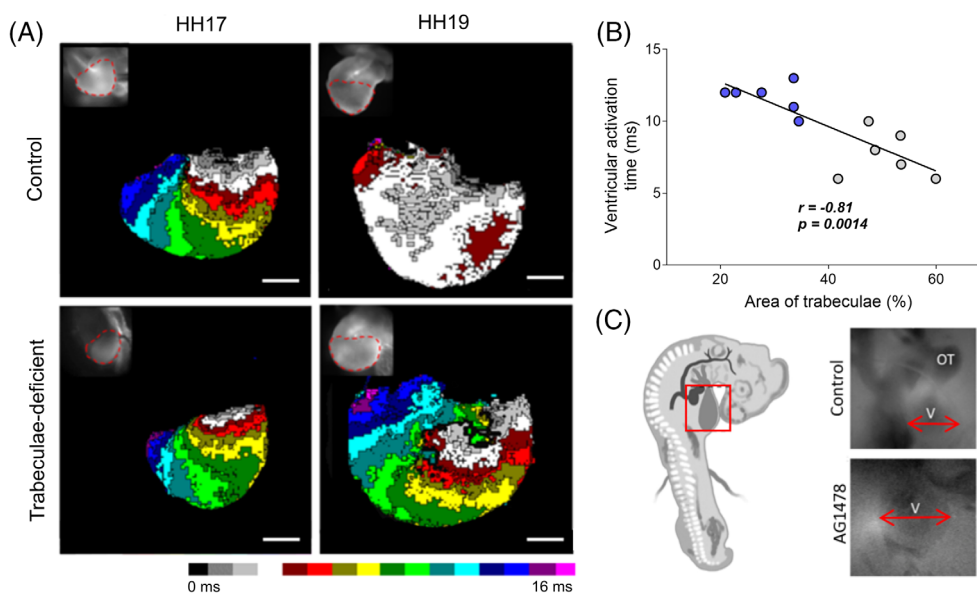


FIGURE 4 Development of ventricular trabeculae correlates with anisotropic conduction pattern and ventricular activation time. The optical map of chick HH17 and HH19 hearts shows the activation pattern transition from slow and isotropic (number and area of colored band per unit of tissue) at the HH17 to the advanced conduction by PIR in control HH18–19 hearts. The AG1478 hearts did not undergo this transition, and an isotropic pattern still activated them even in the HH19 stage ($n = 10$ –13 animals per group at HH17 and 7–26 animals per group at HH18–19, A). The level of ventricular trabeculation at HH18–19 showed a significant negative correlation with the ventricular activation time (B; Pearson's correlation). Trabeculae deficient HH18–19 phenotype was accompanied by important ventricular dilatation compared with controls (red arrow, $n = 7$ –8 per group, C). Scale bar 200 μm ; PIR, primitive interventricular ring.

Nkx2.5^{+/-}, and WT, respectively; $P < 0.001$). Similar to chick model, the significantly decreased in HR was observed in the *Nkx2.5*^{-/-} embryos compared with both *Nkx2.5*^{+/-} and WT (78 ± 9 bpm, 114 ± 9 bpm, and 111 ± 8 bpm for *Nkx2.5*^{-/-}, *Nkx2.5*^{+/-} and WT, respectively; Figure 3L; $P < 0.05$). *ErbB2*^{-/-} mice showed lower the heart rate compared with littermates with at least one WT functional allele (150 ± 15 bpm in *ErbB2*^{-/-} and 163 ± 36 bpm in WT and *ErbB2*^{+/-}, respectively). All genetically targeted mice also model resulted in embryonic mortality.

2.3 | Trabeculae-deficient models revealed isotropic and slow conduction pattern

Next, we addressed the conduction pattern in the trabeculae-deficient ventricle. During development, the heart undergoes a transition of activation sequence from slow isotropic to fast anisotropic. This switch to more advanced anisotropic patterns was observed in control hearts of both pharmacologically inhibited (chick AG1478) and genetically targeted (*Nkx2.5*^{-/-} mouse) models; however, both types of trabeculae-deficient ventricles showed an isotropic conduction sequence. Despite the continuing

embryonic development, no sign of progression to the more advanced conduction pattern was observed in the chick AG1478-treated ventricles (Figure 4A). Both control and AG1478-treated hearts showed a primitive activation pattern with slow isotropic conduction along the ventricle in developmental stage HH17. In the HH18–19 control hearts, 93% of ventricles (24/26) were activated by the advanced PIR sequence (Figure 4A). On the contrary, 7/7 AG1478-treated hearts were activated by the primitive isotropic pattern ($P < 0.001$).

The *Nkx2.5*^{-/-} hearts were activated by a primitive peristaltoid pattern in 100% of cases (17/17; $P < 0.001$); however, the *Nkx2.5*^{+/-} hearts showed a frequency of activation patterns similar to the WT controls (Figure 5A, B). The PIR was present in 78% (11/14) and 91% (10/11) of the *Nkx2.5*^{+/-} and WT embryos, respectively. The left ventricular breakthrough was observed in 3 *Nkx2.5*^{+/-} and 1 WT heart (Figure 5A, B). The *Nkx2.5*^{-/-} ventricle with its primitive activation pattern showed a significantly longer total ventricular activation time compared with both *Nkx2.5*^{+/-} and WT (22.8 ± 8.1 ms in *Nkx2.5*^{-/-} vs 10.4 ± 5.8 ms and 8.0 ± 2.7 ms in *Nkx2.5*^{+/-} and WT, respectively; Figure 5C, $P < 0.05$). In the *ErbB2*-mutated mice line, only a pilot study was performed since the *ErbB2*^{-/-} mice showed a less pronounced electrophysiological phenotype than *Nkx2.5*^{-/-} (Figure 5D, Table S2).

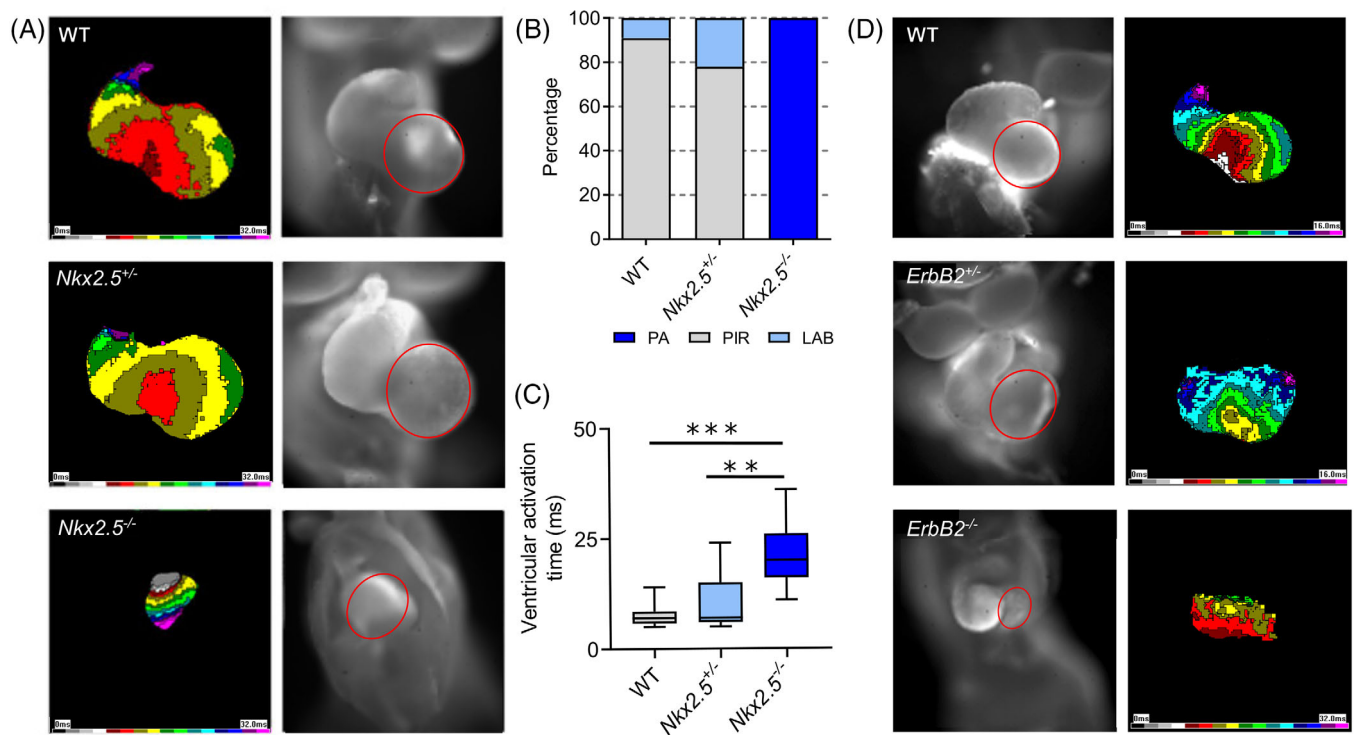


FIGURE 5 Trabeculae-deficient mouse hearts are activated in a slow and isotropic pattern. Panel A shows representative spatiotemporal maps of mouse electrical activation (LV is depicted by the red line in the grayscale image). The ventricular activation by PIR is typically encountered in the WT as well as *Nkx2.5*^{+/-} hearts, while a primitive activation pattern is present in the *Nkx2.5*^{-/-} ventricle. Quantification of ventricular activation patterns showed that while all WT and *Nkx2.5*^{+/-} hearts were activated by advanced conduction sequence (PIR or LAB), ventricles of *Nkx2.5*^{-/-} were activated exclusively by the primitive isotropic pattern, and no advanced activation pattern was observed (B). This was associated with a significant increase in the LV activation time in *Nkx2.5*^{-/-} compared to *Nkx2.5*^{+/-} and WT hearts (C; Kruskal-Wallis test). In all analysis, 10 to 14 animal per group were used. Example of the optical maps of the *ErbB2* mutated mice showing a less pronounced electrophysiological phenotype compared with *Nkx2.5*^{GFP} mice (D). PA, primitive activation along the heart tube; PIR, primary interventricular ring; LAB, left activation breakthrough; LV, left ventricle. Data expressed as mean \pm SD; ** $P < 0.001$ and *** $P < 0.0001$ vs *Nkx2.5*^{-/-}. All pictures in panels A and D are at the same magnification (10 \times water immersion objective).

2.4 | Acceleration of ventricular conduction in early cardiogenesis correlates with the level of trabeculation in chick trabeculae-deficient hearts

We observed that AG1478-induced trabecular inhibition did not produce a ventricle with a completely smooth wall, rather creating a phenotype with rudimentary trabeculae (trabecular area: $28.8 \pm 6.0\%$ in AG1478 treated vs $50.8 \pm 2.5\%$ in control; Figure 3I, $P < 0.0001$). This finding is similar to an observation about the not entirely absent trabecular system, but rather arrested at the stage of their emergence as reported previously in AG1478-treated zebrafish or even in some of the neuregulin pathway-targeted mouse. Some of these models also showed an important degree of phenotype variation.^{19–22} Therefore, we took an advantage of the phenotype variability and correlated the degree of trabecular development with ventricular conduction time. Analyzing both control and AG1478-treated hearts, we showed a significant negative correlation between the level of developed

trabecular area and time of ventricular activation (Figure 4B; $P = 0.0014$). This implies that the less level of trabeculation, the slower ventricular activation was. We were not able to perform a similar correlation analysis in the mouse models since they do not possess enough level of phenotypes variation. Although the significant reduction of a trabecular layer of the ventricle was observed in both null mice compared with WT (trabecular area: $31.2 \pm 6.1\%$ vs $59.0 \pm 6.3\%$ for *Nkx2.5*^{-/-} and WT, respectively, $P < 0.0001$, Figure 3K; and 19.2 ± 2.0 vs $35.8 \pm 5.3\%$ for *ErbB2*^{-/-} and WT, respectively, $P < 0.001$), the development of trabeculae in the heterozygotes did not allow the correlation analysis.

2.5 | Ventricle of *ErbB2*^{-/-} mouse expresses Cx40

To determine the potential role of the chamber myocardium differentiation on the observed slow conduction phenotype, we employed the *ErbB2*^{-/-} mice. Heterodimer

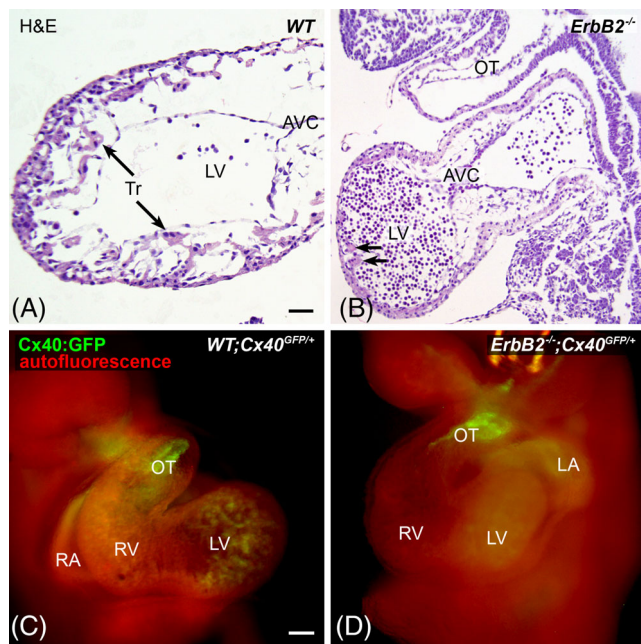


FIGURE 6 *ErbB2*^{-/-} embryonic hearts with rudimentary trabeculae express Cx40. Representative image of WT (A) and *ErbB2*^{-/-} (B) mouse hearts at ED9.75 showing a dramatic reduction in the trabecular network (arrows) in the *ErbB2*^{-/-} hearts. The level of green fluorescence was comparable in the OT endocardium and atria between the WT;*Cx40*^{GFP/+} (C) and *ErbB2*^{-/-};*Cx40*^{GFP/+} (D) embryos. Quantification of GFP fluorescence in the left ventricle showing comparable level between *ErbB2*^{-/-};*Cx40*^{GFP/+} and *ErbB*^{+/-};*Cx40*^{GFP/+} (n = 2-3 animals per group, E). AVC, atrioventricular canal; LA, left atrium; LV, left ventricle; RA, right atrium; RV, right ventricle; OT, outflow tract; Tr, ventricular trabeculae. Scale bar 100 μm (same between panels A and B, and C and D, respectively).

ErbB2/*ErbB4*, as a neuregulin receptor, is a crucial component of the Neuregulin/*ErbB* signaling pathway.²⁰ *ErbB2*^{-/-} mice have a deletion of one of the nonredundant myocardial receptors for neuregulin. Unlike the other mice with deletion of neuregulin itself or its receptor *ErbB4*, which do not survive past ED9.5, these mice survive up to ED9.75²³ The embryos showed a drastic reduction in the trabecular layer of the ventricular wall compared to the WT littermates (Figure 6A, B). By crossing this line to the *Cx40*^{GFP} background,²⁴ we were able to study the expression of Cx40 (as a hallmark of the chamber specification into the faster conduction myocardium) even before possible Cx40 detection by immunohistochemistry (up ED10).²⁵ The level of green fluorescence in the atria and outflow tract endocardium was similar between genotypes in all four cases of *ErbB2*^{-/-};*Cx40*^{GFP/+} and comparable with the level observed in the WT;*Cx40*^{GFP/+} hearts (Figure 6C, D). The intensity of *Cx40*^{GFP} fluorescence in the ventricle was not significantly different between *ErbB2*^{-/-};*Cx40*^{GFP/+} and

ErbB2^{+/-};*Cx40*^{GFP/+} (98 ± 8 vs 95 ± 16 in *ErbB2*^{-/-};*Cx40*^{GFP/+} and *ErbB2*^{+/-};*Cx40*^{GFP/+}, respectively, $P = 0.73$).

3 | DISCUSSION

In this work, we focused on the function of the trabecular system in impulse spreading in the early developing endothermic heart. In the looping heart, using either simulation of the impulse propagation inside the ventricle or direct endocardial surface imaging, we showed that trabeculae development is associated with an anisotropic conduction pattern allowing earlier apex activation.

Despite the obvious morphological similarities, ventricles of ectotherms differ from embryonic mammalian and avian trabecular ventricle designs. Adult mammalian and avian hearts work under higher pressure than ectothermic ones,²⁶⁻²⁸ and their highly trabeculated embryonic ventricles represent only an intermittent stage. While hemodynamic loading represents an important factor in trabeculae formation,^{20,29} the question about the similar morphology to the functional relationship has been raised. This needs to be considered bearing in mind that the intraventricular pressure in the embryonic heart of endotherms is lower than in the adult ones.³⁰⁻³² Moreover, the initial steps in trabecular formation differ in the prototypical ectothermic (zebrafish) and endothermic (mouse and chick) heart.^{17,33,34} Variation also exists in the level of trabeculation. In the adult ectotherms, the trabecular proportions encompass around 80% of the ventricular wall instead of 40% to 50% in the case of ED4 chick heart.²⁷

Concerning the role of ventricular trabeculae in the impulse spreading, interconnection of the trabecular system at the atrioventricular junction with the apical part of the ventricle in *Xenopus laevis* was reported. This connection was associated with the first epicardial activation near the ventricular apex and was interpreted as a functional analog of the specialized ventricular conduction tissue.^{12,13} Similar findings were reported in frog hearts.³⁵ Interestingly, intraventricular conduction by trabeculae is not linked with univentricular design (common in the ectothermic heart) only since it was observed in reptile hearts with the complete ventricular septum (alligator, crocodile) as well.^{36,37} The potentially confusing fact that the apex-first activation is not universal in all ectothermic species³⁸⁻⁴⁰ could be attributed to the high level of variation in the ventricular architecture and trabecular organization.^{27,38,41,42}

The unresolved question is whether the trabeculae in endotherms also lead to the anisotropy of impulse conduction inside the early-developed ventricle. This assumption was proposed already by Viragh and Challice

based on morphological observation of trabecular arrangement.⁴³ The first attempt at indirect confirmation of this assumption came from the study of de Jong and colleagues. Using bipolar electrode measurements in the HH31 chick embryonic heart showed fractionalized epicardial electrogram and considered the first deflection as depolarization of the trabecular network. This led them to suggest that trabecular activation precedes the ones of the outer compact ventricular wall.⁷ However, HH31 hearts are highly compacted and thus prevent a clear distinction between the trabecular and compact layer of the ventricular wall. In the present study, the employment of the earlier stages of the developing ventricle allowed us to localize activation waves more precisely within the trabecular network. We used a model of impulse propagation adapted to the embryonic ventricle.¹⁶ Simulated activation maps assuming a constant activation speed along the developing structures (both ventricular wall and trabecular network) showed earlier apex activation in the trabeculated dataset than in the trabeculae-deficient ventricle, implying that trabeculae provided a shortcut for the apex activation. This role of trabeculae was confirmed by earlier activation of the trabeculae compared to the ventricular wall in the opened chick ED4 heart. Activation in the trabecular network was clearly shown to precede the rest of the surrounding tissue. This signal could not be attributed to the wall activation since it was not observed in the uncut hearts. These findings suggest that in the early endothermic hearts, the depolarization wave was spread preferentially through the embryonic trabecular network, similar to some ectotherms.

Considering the role of the trabecular network in intraventricular conduction, we further analyzed the conduction in two examples of the trabeculae-deficient ventricle. In the first model, we targeted the Neuregulin/ErbB signaling. This pathway was shown to be a key pathway for trabeculation in both ectotherms and endotherms.^{33,44,45} Disruption of Neuregulin/ErbB signaling by AG1478 was reported to create a phenocopy with loss of neuregulin signaling⁴⁶⁻⁴⁸ and to produce trabeculae-deficient heart in zebrafish.^{19,20} Interestingly, a recent study showed that atrial cardiomyocytes of zebrafish, like ventricular cardiomyocytes, can respond to Nrg2a/ErbB2 signaling as well.²¹ Similar to our findings, this study showed timescale as an essential factor for proper Neuregulin/ErbB signaling disruption. Here we determined the window for the chick ventricle at around 62 hours of incubation. This time frame clearly corresponds with trabecular emergence in chick hearts.^{17,18} We have shown slow and isotropic conduction sequence with no progression to the advance activation patterns in the chick AG1478-induced trabeculae-deficient hearts.

The second model of the trabeculae-deficient ventricle was created by genetic ablation of *Nkx2.5*, a transcription factor governing the cardiomyocyte differentiation program. The heterozygous state led to the cardiac conduction system hypoplasia, while its complete deletion is embryonic lethal around ED10.⁴⁷ The weak and atypical contraction sequence was described in the ED9.5 *Nkx2.5*^{-/-} hearts.⁴⁹ The authors correlated this with the observed broad AVC and possible retrograde blood flow.⁴⁹ The role of *Nkx2.5* in the development of pacemaker is controversial. Earlier studies thought that *Nkx2.5* is excluded from the developing sinoatrial node (SAN)⁵⁰ and its expression in SAN or pulmonary sleeves prevents myocardium from pacemaker activity.^{51,52} However, a recent study has shown that the *Nkx2.5* is expressed in the SAN junction^{53,54} and plays a role in the development of a subpopulation of pacemaker cells.⁵⁵ *Nkx2.5* inactivation in SAN junction thus led to the SAN dysfunction.⁵⁵ We and others observed decreased heart rate in the *Nkx2.5*^{-/-} embryos.⁴⁹ Since the heart rate physiologically increases during early mouse development,^{56,57} the decreased heart rate could be also the result of developmental delay observed in *Nkx2.5*^{-/-} embryos. Alternatively, decreased perfusion due to low cardiac output caused by a slower heart rate could lead to embryonic growth retardation and ultimate demise, as seen in the pharmacological intervention model (ivabradine) in the chick embryo.⁵⁸ Considering the conduction pattern, similarly as in the AG1478-treated chick, *Nkx2.5*^{-/-} trabeculae-deficient ventricles failed to progress to the advanced activation pattern and showed a slow and isotropic conduction pattern. Accordingly, the decrease of ventricular activation time presented during physiological development concomitantly with activation pattern progression⁹ was not observed.

Since the *Nkx2.5* deletion was reported to dysregulate the cardiac connexins,^{49,59-61} their depletion could affect the conduction speed in *Nkx2.5*^{-/-} hearts. To define the role of the fast conduction myocardium maturation in the observed slow conduction of the trabeculae-deficient ventricles, the *ErBb2*^{-/-}; *Cx40*^{GFP/+} was subsequently analyzed. The *ErBb2*^{-/-}; *Cx40*^{GFP/+} ventricle slowed the presence of green fluorescence implying unaltered *Cx40* expression. Thus, it can be assumed that the Neuregulin/ErbB pathway does not affect *Cx40* expression. Moreover, our simulation data considering spatial dimensions only (without any changes related to the connexins or ion channel expression), showed that the trabeculae network is sufficient to provide a shortcut to apex activation. Altogether, these findings suggest that the observed slow epicardial conduction of trabeculae-deficient hearts could be attributed to severely affected trabecular architecture rather than absent *Cx40* expression.

In addition to the slow conduction pattern presented in both trabeculae-deficient models, in the AG1478-induced trabeculae-deficient chick hearts we showed a significant negative correlation between the total ventricular activation time and trabecular development level. Collectively, these findings strongly suggest that the early trabecular development forms a substrate for preferential impulse propagation and is essential for the proper activation patterning. Ventricular dilatation, probably due to insufficient wall stiffness observed in the trabeculae-deficient AG1478-treated hearts, resulted in altered contractility and ultimately led to heart failure and embryonic death. We cannot fully exclude the role of possible insufficient AVC valve function with consequent retrograde flow to the atria, similarly as reported in *Nkx2.5*^{-/-} animals,⁴⁹ in altered contractility observed of these hearts. On the other hand, in case of AG1478-induced trabeculae-deficient heart, no cardiac valve defect was reported in the zebrafish.¹⁹ Moreover, it is highly unlikely that the altered AV valve function with preserved ventricular contractility would result in important ventricular dilatation. Since we observed dilated ventricle with weak contraction, we attributed the altered contractile function in the AG1478-treated hearts to the inability of trabeculae-deficient hearts to develop a mature conduction system with a consequent inadequate adaptation of the pumping function. This together with a thin ventricular wall resulted in ventricular dilatation. Similar findings of impaired contractility after AG1478 treatment was reported in the zebrafish hypotrabeulaed model.²⁰

4 | CONCLUSION

Our results showed that, in addition to other functions in the developing heart, the trabeculae are essential in establishing a preferential conduction pathway inside the forming ventricle and conduction patterning. Lack of trabeculae then leads to failure of conduction parameters differentiation and decline in contractility (in AG1478-induced model), resulting in primitive peristaltoid ventricular activation with consequent embryonic heart failure.

5 | EXPERIMENTAL PROCEDURES

All procedures performed on animals were in accordance with the ethical standards of Charles University and were approved by the Animal Care and Use Committee of the First Faculty of Medicine.

5.1 | Experimental models

5.1.1 | Mouse models

The *Nkx2.5*^{GFP} knock-in⁶² at ED9.5 was used for genetic ablation of trabecular development. *ErbB2*^{-/-} mice at ED9.75 were used to produce hearts with substantial trabecular reduction targeting Neuregulin/ErbB pathway. The breeding pairs were caged overnight, and the noon of the day when the plug was discovered was considered ED 0.5. Time-pregnant females were sacrificed at the appropriate time, and the embryos were rapidly dissected. The *Nkx2.5*^{+/-} and *Nkx2.5*^{-/-} genotype was confirmed by detecting GFP using an epifluorescence microscope fitted with the appropriate filter set (Olympus, Tokyo, Japan). The genotype of *ErbB2*^{-/-} mice was confirmed by PCR as described.²³ In addition, *ErbB2*^{-/-} mice were crossed with the *Cx40*^{GFP} line to visualize *Cx40* expression.²⁴ *Cx40*^{GFP} mice with Swiss albino background were used as a control. The CRL was measured directly after embryos dissection.

5.1.2 | Chick trabeculae deficient heart

In chick, the Neuregulin/ErbB pathway was targeted by applying the AG1478, an inhibitor of the theErbB1 receptor, and the ErbB2/ErbB3 heterodimer.²⁰ We adjusted the protocol previously described for zebrafish¹⁹ to the chick embryos. White Leghorn chicken eggs incubated for 62 hours were windowed on the blunt end, and AG1478 (Sigma Aldrich; 90 pg in 18 μ L DMSO, diluted to 200 μ L by physiological saline) was applied adjacent to the developing vasculature. Controls received DMSO with physiological saline solution. The shell was closed with the Scotch tape, and the eggs were re-incubated to the desired HH stage 17 and 18, 19, respectively.^{14,63} At HH18-19, the phenotype was fully developed (ventricular dilatation, weak contraction), and at the same time, embryos were still alive to enable electrical and mechanical function assessment.

5.2 | Methods

5.2.1 | Simulation of impulse propagation

The chick trabeculae-deficient hearts were generated as described above. At HH19, AG1478 treated and control hearts were isolated, fixed with 4% paraformaldehyde in phosphate buffer saline (PBS), and scanned using an ex vivo micro-CT (SkyScan 1272, Bruker Micro-CT, Belgium). Before scanning, specimens were X-ray

contrasted by phosphotungstic acid according to the protocol described by Metscher.⁶⁴ Each specimen was placed in a plastic tube with PBS and scanned with the following parameters: pixel size 2 μm , source voltage 60 kV, source current 166 mA, rotation step 0.4, no filter, 180° rotation. After pre-processing, the data volume was thresholded by a Gaussian filter using Amira 2020.1 software (Thermo Fisher Scientific, Waltham, Massachusetts, USA). The geodesic distance¹⁵ from the AVC to the ventricle border was further calculated and visualized by color on the triangulated surface of the heart. Three trabeculae-deficient and control hearts were used for analysis.

5.2.2 | Optical mapping

The freshly isolated hearts (Nkx2.5 mutated mice: ED 9.5, $n = 14$ for *Nkx2.5*^{-/-}, 11 for *Nkx2.5*^{+/-} and 10 for WT; ErbB2 mutated mice: ED9.75, $n = 4$ for *ErbB2*^{-/-}, 11 for *ErbB2*^{+/-} and 7 for WT; chick: $n = 13$ for AG1478 treated and 10 for control at HH17 and 7 for AG1478 and 26 for control at HH18-19, respectively) were rapidly dissected and stained by voltage-sensitive dye di-4-ANNEPS (ThermoFisher Scientific; 1.7 mM) in 4°C Tyrode's solution for 5 minutes. To reduce motion artifacts, Blebbistatin (Sigma Aldrich; 0.1 μM) was added to the solution before imaging. Mapping of epicardial electrical activity was performed in spontaneously beating hearts immersed in warm (37°C) Tyrode solution (composition in mmol/l: NaCl 145, NaCl 145, 5.9 KCl, 1.1 CaCl₂, 1.2 MgCl₂, 11 glucose, 5 HEPES; pH = 7.4; gassed with 100% O₂) using the Ultima L high-speed camera (SciMedia Ltd., Tokyo, Japan) fitted to a BX51 FS epifluorescence microscope (Olympus, Japan) and equipped with a 150 W Xe arc lamp (Cairn, UK).

Subsequent analysis was performed using the software BV_ANA bundled with the camera as described previously.^{65,66} We analyzed heart rate, spatiotemporal reconstruction of activation pattern, total ventricular activation time, and location of the first ventricular activation site.

Mapping of electrical activity in the endocardial aspects was performed in chick ED4 hearts (HH24; $n = 5$). After whole heart mapping, the ventricle was dissected in the frontal plane under the SZH 10 stereomicroscope (Olympus, Japan) to view the dorsal half of the heart with the endocardial trabeculae surface.²⁹ Hearts were pinned endocardial side up in a custom-made Sylgard chamber in the position parallel with the objective lens to prevent heart edges to coil and enable mapping of the activation pattern of the whole endocardial surface trabeculae. All hearts were stable in beating frequency for the entire imaging time. Mapping and analysis were performed as described above.

5.2.3 | Analysis of contractility

To assess the contractile function of HH19 hearts ($n = 7$ for AG1478 treated and $n = 8$ for controls), the *in-ovo* videomicroscopy was performed as described previously.⁶⁷ The embryos *in ovo* were maintained at 37°C using a custom-made Styrofoam-insulated metal container filled with pre-heated Bath Armor pellets placed on a Torrey Pines Scientific chilling/heating plate. Ten-second movies were recorded with a Nikon D7000 camera (640 x 480 px, 30 fps) mounted on a Leica 125 dissecting microscope; for illumination, a 150 W halogen light source was fitted with a green interference filter to enhance blood contrast, was used. Ventricular dimensions during the whole cardiac cycle and contractility were subsequently assessed.

5.2.4 | Quantitative analysis

After optical mapping, the Nkx2.5^{GFP} hearts were fixed in 4% (wt/vol) in paraformaldehyde in PBS, optically cleared using CUBIC2,⁶⁸ and subjected to whole-mount microscopy with 4x or 10x objectives and 10 or 2.5 μm z-steps using FluoView FV1000 confocal system fitted on an upright BX61 microscope (Olympus, Tokyo, Japan). Chick hearts were imaged in the same way using endogenous autofluorescence instead of GFP.⁶⁹ To analyze the area of the trabecular network, the maximal ventricular diameter was found in the 3D data set and analyzed in FIJI software (NIH, USA). The threshold was set to exclude blood and include the outer ventricular wall with the entire trabecular network. In the ROI delineated by the atrioventricular cushions on one side and the outflow cushions on the opposite side, the trabecular area was then calculated as a percentage of an outer ventricular wall from ROI. Hearts of *ErbB2*^{-/-} and WT littermates were processed for paraffin embedding and sectioned at 7 μm . Hematoxylin and eosin staining was further performed to reveal ventricular wall morphology. The extent of the trabecular network was analyzed as described above. In all quantitative analyses $n = 3$ to 7 per group. Whole heart fluorescence imaging of optically cleared ErbB2 mice at Cx40 background was performed to analyze GFP fluorescence as a proxy for connexin40 expression. Specific GFP fluorescence was measured after background subtractions. The mean intensity of green channel fluorescence was analyzed in five different areas of the left ventricular myocardium spanning the entire ventricle in FIJI software (NIH, USA) using a sampling square of 10 × 10 pixels ($n = 2$ -3 mice per group).

5.2.5 | Statistical analysis

GraphPad Prism 9 (GraphPad Software, Inc., San Diego, CA) was used for graphic presentation and statistical analysis. Normality of data distribution was tested by Shapiro-Wilk test. Unpaired Student's *t*-test or one-way ANOVA and subsequent Student-Newman-Keuls test were used to compare differences in normally distributed variables between groups. Mann-Whitney or Kruskal-Wallis test was used to compare differences in non-normally variables between groups (analysis of ventricular activation time and CRL). The Chi-square test was used to compare activation patterns frequency among the groups. Pearson's correlation coefficient was used for correlation analyses. Differences were considered statistically significant when $P < .05$.

AUTHOR CONTRIBUTIONS

Veronika Olejnickova: Conceptualization (equal); funding acquisition (equal); investigation (equal); methodology (equal); project administration (lead); resources (lead); supervision (equal); validation (equal); writing – original draft (equal); writing – review and editing (equal). **Peter Uriel Hamor:** Investigation (equal). **Jiri Janacek:** Methodology (equal); software (lead); validation (equal); visualization (equal); writing – original draft (equal). **Martin Bartos:** Investigation (equal); methodology (equal); writing – original draft (equal). **Eva Zaborodska:** Investigation (equal). **Barbora Sankova:** Investigation (equal); methodology (equal). **Alena Kvasilova:** Investigation (equal); methodology (equal). **Hana Kolesova:** Investigation (equal). **David Sedmera:** Conceptualization (equal); funding acquisition (equal); methodology (equal); supervision (equal); validation (equal); writing – original draft (equal); writing – review and editing (equal).

ACKNOWLEDGEMENTS

The authors thank Ms. Blanka Topinkova and Jarmila Svatakova for their excellent technical assistance and Mr. Ivan Helekal for the drawing (Figure 4C). The authors would also like to express their sincere thanks to Dr. Richard Harvey (Victor Chang Cardiac Research Institute, Australia) for providing the Nkx2.5^{GFP} mouse line and Dr. C. Birchmeier (Max-Delbrück-Center for Molecular Medicine, Berlin, Germany) for providing the ErbB2 mutated mouse line. The graphical abstract was created using Biorender.

ORCID

Veronika Olejnickova  <https://orcid.org/0000-0002-0991-1420>

Jiri Janacek  <https://orcid.org/0000-0003-0286-4999>

Martin Bartos  <https://orcid.org/0000-0002-1998-0278>

Barbora Sankova  <https://orcid.org/0000-0001-6560-1286>

Alena Kvasilova  <https://orcid.org/0000-0002-2399-0428>

Hana Kolesova  <https://orcid.org/0000-0003-1861-9445>

David Sedmera  <https://orcid.org/0000-0002-6828-3671>

REFERENCES

1. Moorman AFM, Christoffels VM. Development of the cardiac conduction system: a matter of chamber development. *Novartis Found Symp.* 2003;250:25-34. discussion 34–43, 276–279.
2. Kamino K, Hirota A, Fujii S. Localization of pacemaking activity in early embryonic heart monitored using voltage-sensitive dye. *Nature.* 1981;290(5807):595-597. doi:10.1038/290595a0
3. Hirota A, Kamino K, Komuro H, Sakai T, Yada T. Early events in development of electrical activity and contraction in embryonic rat heart assessed by optical recording. *J Physiol.* 1985;369:209-227. doi:10.1113/jphysiol.1985.sp015897
4. Christoffels VM, Burch JBE, Moorman AFM. Architectural plan for the heart: early patterning and delineation of the chambers and the nodes. *Trends Cardiovasc Med.* 2004;14(8):301-307. doi:10.1016/j.tcm.2004.09.002
5. Chuck ET, Freeman DM, Watanabe M, Rosenbaum DS. Changing activation sequence in the embryonic chick heart. Implications for the development of the his-Purkinje system. *Circ Res.* 1997;81(4):470-476. doi:10.1161/01.res.81.4.470
6. Chuck ET, Meyers K, France D, Creazzo TL, Morley GE. Transitions in ventricular activation revealed by two-dimensional optical mapping. *Anat Rec.* 2004;280A(2):990-1000. doi:10.1002/ar.a.20083
7. de Jong F, Opthof T, Wilde AA, et al. Persisting zones of slow impulse conduction in developing chicken hearts. *Circ Res.* 1992;71(2):240-250.
8. Rentschler S, Vaidya DM, Tamaddon H, et al. Visualization and functional characterization of the developing murine cardiac conduction system. *Development.* 2001;128(10):1785-1792.
9. Sankova B, Benes J, Krejci E, et al. The effect of connexin40 deficiency on ventricular conduction system function during development. *Cardiovasc Res.* 2012;95(4):469-479. doi:10.1093/cvr/cvs210
10. Sedmera D, Reckova M, Bigelow MR, et al. Developmental transitions in electrical activation patterns in chick embryonic heart. *Anat Rec.* 2004;280A(2):1001-1009. doi:10.1002/ar.a.20107
11. Challice CE, Virágh S. The phylogenetic and ontogenetic development of the mammalian heart: some theoretical considerations. *Acta Biochim Biophys Acad Sci Hung.* 1974;9(1-2):131-140.
12. Arbel ER, Liberthson R, Langendorf R, Pick A, Lev M, Fishman AP. Electrophysiological and anatomical observations on the heart of the African lungfish. *Am J Physiol.* 1977;232(1):H24-H34. doi:10.1152/ajpheart.1977.232.1.H24
13. Sedmera D, Reckova M, de Almeida A, et al. Functional and morphological evidence for a ventricular conduction system in zebrafish and Xenopus hearts. *Am J Physiol Heart Circ Physiol.* 2003;284(4):H1152-H1160. doi:10.1152/ajpheart.00070.2002
14. Hamburger V, Hamilton HL. A series of normal stages in the development of the chick embryo. 1951. *Dev Dyn.* 1992;195(4):231-272. doi:10.1002/aja.1001950404

15. Lantuejoul C, Beucher S. On the use of the geodesic metric in image analysis. *J Microsc.* 1981;121(1):39-49. doi:10.1111/j.1365-2818.1981.tb01197.x
16. Olejnickova V, Sankova B, Sedmera D, Janacek J. Trabecular architecture determines impulse propagation through the early embryonic mouse heart. *Front Physiol.* 2018;9:1876. doi:10.3389/fphys.2018.01876
17. Icardo JM, Fernandez-Terán A. Morphologic study of ventricular trabeculation in the embryonic chick heart. *Acta Anat (Basel).* 1987;130(3):264-274. doi:10.1159/000146455
18. Sedmera D, Pexieder T, Hu N, Clark EB. Developmental changes in the myocardial architecture of the chick. *Anat Rec.* 1997;248(3):421-432. doi:10.1002/(SICI)1097-0185(199707)248:3<421::AID-AR15>3.0.CO;2-R
19. Liu J, Bressan M, Hassel D, et al. A dual role for ErbB2 signaling in cardiac trabeculation. *Development.* 2010;137(22):3867-3875. doi:10.1242/dev.053736
20. Peshkovsky C, Totong R, Yelon D. Dependence of cardiac trabeculation on neuregulin signaling and blood flow in zebrafish. *Dev Dyn.* 2011;240(2):446-456. doi:10.1002/dvdy.22526
21. Rasouli SJ, Stainier DYR. Regulation of cardiomyocyte behavior in zebrafish trabeculation by Neuregulin 2a signaling. *Nat Commun.* 2017;8(1):15281. doi:10.1038/ncomms15281
22. Donna L, Xifu L, Ariel F, et al. Neuregulin 1 sustains the gene regulatory network in both trabecular and nontrabecular myocardium. *Circ Res.* 2010;107(6):715-727. doi:10.1161/CIRCRESAHA.110.218693
23. Britsch S, Li L, Kirchhoff S, et al. The ErbB2 and ErbB3 receptors and their ligand, neuregulin-1, are essential for development of the sympathetic nervous system. *Genes Dev.* 1998;12(12):1825-1836. doi:10.1101/gad.12.12.1825
24. Miquerol L, Meysen S, Mangoni M, et al. Architectural and functional asymmetry of the his-Purkinje system of the murine heart. *Cardiovasc Res.* 2004;63(1):77-86. doi:10.1016/j.cardiores.2004.03.007
25. Sedmera D, Reckova M, DeAlmeida A, et al. Spatiotemporal pattern of commitment to slowed proliferation in the embryonic mouse heart indicates progressive differentiation of the cardiac conduction system. *Anat Rec.* 2003;274A(1):773-777. doi:10.1002/ar.a.10085
26. Jensen B, van der Wal AC, Moorman AFM, Christoffels VM. Excessive trabeculations in noncompaction do not have the embryonic identity. *Int J Cardiol.* 2017;227:325-330. doi:10.1016/j.ijcard.2016.11.089
27. Jensen B, Agger P, de Boer BA, et al. The hypertrabeculated (noncompacted) left ventricle is different from the ventricle of embryos and ectothermic vertebrates. *Biochim Biophys Acta.* 2016;1863((7, Part B)):1696-1706. doi:10.1016/j.bbamcr.2015.10.018
28. Joyce W, Wang T. What determines systemic blood flow in vertebrates? *J Exp Biol.* 2020;223(4):1-15. doi:10.1242/jeb.215335
29. Reckova M, Rosengarten C, de Almeida A, et al. Hemodynamics is a key epigenetic factor in development of the cardiac conduction system. *Circ Res.* 2003;93(1):77-85. doi:10.1161/01.RES.0000079488.91342.B7
30. Clark EB, Hu N, Dummett JL, Vandekieft GK, Olson C, Tomanek R. Ventricular function and morphology in chick embryo from stages 18 to 29. *Am J Physiol.* 1986;250(3 Pt 2):H407-H413. doi:10.1152/ajpheart.1986.250.3.H407
31. Girard H. Arterial pressure in the chick embryo. *Am J Physiol.* 1973;224(2):454-460. doi:10.1152/ajplegacy.1973.224.2.454
32. Struijk PC, Mathews VJ, Loupas T, et al. Blood pressure estimation in the human fetal descending aorta. *Ultrasound Obstet Gynecol.* 2008;32(5):673-681. doi:10.1002/uog.6137
33. Del Monte-Nieto G, Ramalison M, Adam AAS, et al. Control of cardiac jelly dynamics by NOTCH1 and NRG1 defines the building plan for trabeculation. *Nature.* 2018;557(7705):439-445. doi:10.1038/s41586-018-0110-6
34. Staudt DW, Liu J, Thorn KS, Stuurman N, Liebling M, Stainier DYR. High-resolution imaging of cardiomyocyte behavior reveals two distinct steps in ventricular trabeculation. *Development.* 2014;141(3):585-593. doi:10.1242/dev.098632
35. Abramochkin DV, Rozenshtaukh LV. Optical mapping of chronotopography of excitation of the frog heart ventricle epicardial surface in sinus rhythm. *Russ Fiziol Zh Im I M Sechenova.* 2008;94(4):414-420.
36. Jensen B, Boukens BJ, Crossley DA II, et al. Specialized impulse conduction pathway in the alligator heart. *eLife.* 2018;7:e32120. doi:10.7554/eLife.32120
37. Kvasilova A, Olejnickova V, Jensen B, et al. The formation of the atrioventricular conduction axis is linked in development to ventricular septation. *J Exp Biol.* 2020;223(Pt 19):1-5. doi:10.1242/jeb.229278
38. Jensen B, Boukens BJD, Postma AV, et al. Identifying the evolutionary building blocks of the cardiac conduction system. *PLoS One.* 2012;7(9):e44231. doi:10.1371/journal.pone.0044231
39. Vaykshnorayte MA, Azarov JE, Tsvetkova AS, Vityazev VA, Ovechkin AO, Shmakov DN. The contribution of ventricular apicobasal and transmural repolarization patterns to the development of the T wave body surface potentials in frogs (*Rana temporaria*) and pike (*Esox lucius*). *Comp Biochem Physiol A Mol Integr Physiol.* 2011;159(1):39-45. doi:10.1016/j.cbpa.2011.01.016
40. Vityazev VA, Azarov JE. Stretch-excitation correlation in the toad heart. *J Exp Biol.* 2020;223(Pt 23):1-5. doi:10.1242/jeb.228882
41. Jensen B, Moorman AFM, Wang T. Structure and function of the hearts of lizards and snakes. *Biol Rev Camb Philos Soc.* 2014;89(2):302-336. doi:10.1111/brv.12056
42. Stephenson A, Adams JW, Vaccarezza M. The vertebrate heart: an evolutionary perspective. *J Anat.* 2017;231(6):787-797. doi:10.1111/joa.12687
43. Virágh S, Challice CE. The development of the conduction system in the mouse embryo heart. I. the first embryonic A-V conduction pathway. *Dev Biol.* 1977;56(2):382-396.
44. Rentschler S, Zander J, Meyers K, et al. Neuregulin-1 promotes formation of the murine cardiac conduction system. *Proc Natl Acad Sci U S A.* 2002;99(16):10464-10469. doi:10.1073/pnas.162301699
45. Samsa LA, Yang B, Liu J. Embryonic cardiac chamber maturation: Trabeculation, conduction and Cardiomyocyte proliferation. *Am J Med Genet C Semin Med Genet.* 2013;163(3):157-168. doi:10.1002/ajmg.c.31366
46. Budi EH, Patterson LB, Parichy DM. Embryonic requirements for ErbB signaling in neural crest development and adult pigment pattern formation. *Development.* 2008;135(15):2603-2614. doi:10.1242/dev.019299

47. Lyons DA, Pogoda HM, Voas MG, et al. *erbb3* and *erbb2* are essential for Schwann cell migration and myelination in zebrafish. *Curr Biol*. 2005;15(6):513-524. doi:10.1016/j.cub.2005.02.030
48. Scherz PJ, Huisken J, Sahai-Hernandez P, Stainier DYR. High-speed imaging of developing heart valves reveals interplay of morphogenesis and function. *Development*. 2008;135(6):1179-1187. doi:10.1242/dev.010694
49. Dupays L, Jarry-Guichard T, Mazurais D, et al. Dysregulation of connexins and inactivation of NFATc1 in the cardiovascular system of *Nkx2-5* null mutants. *J Mol Cell Cardiol*. 2005;38(5):787-798. doi:10.1016/j.yjmcc.2005.02.021
50. Christoffels VM, Mommersteeg MTM, Trowe MO, et al. Formation of the venous pole of the heart from an *Nkx2-5*-negative precursor population requires *Tbx18*. *Circ Res*. 2006;98(12):1555-1563. doi:10.1161/01.RES.0000227571.84189.65
51. Ye W, Wang J, Song Y, et al. A common *Shox2-Nkx2-5* antagonistic mechanism primes the pacemaker cell fate in the pulmonary vein myocardium and sinoatrial node. *Development*. 2015;142(14):2521-2532. doi:10.1242/dev.120220
52. Espinoza-Lewis RA, Liu H, Sun C, Chen C, Jiao K, Chen Y. Ectopic expression of *Nkx2.5* suppresses the formation of the sinoatrial node in mice. *Dev Biol*. 2011;356(2):359-369. doi:10.1016/j.ydbio.2011.05.663
53. Liang X, Wang G, Lin L, et al. *HCN4* dynamically marks the first heart field and conduction system precursors. *Circ Res*. 2013;113(4):399-407. doi:10.1161/CIRCRESAHA.113.301588
54. Wiese C, Grieskamp T, Airik R, et al. Formation of the sinus node head and differentiation of sinus node myocardium are independently regulated by *Tbx18* and *Tbx3*. *Circ Res*. 2009;104(3):388-397. doi:10.1161/CIRCRESAHA.108.187062
55. Li H, Li D, Wang Y, et al. *Nkx2-5* defines a subpopulation of pacemaker cells and is essential for the physiological function of the sinoatrial node in mice. *Development*. 2019;146(14):dev178145. doi:10.1242/dev.178145
56. Keller BB, MacLennan MJ, Tinney JP, Yoshigi M. In vivo assessment of embryonic cardiovascular dimensions and function in day-10.5 to -14.5 mouse embryos. *Circ Res*. 1996;79(2):247-255. doi:10.1161/01.res.79.2.247
57. Phoon CKL, Ji RP, Aristizábal O, et al. Embryonic heart failure in *NFATc1*^{-/-} mice: novel mechanistic insights from in utero ultrasound biomicroscopy. *Circ Res*. 2004;95(1):92-99. doi:10.1161/01.RES.0000133681.99617.28
58. Kockova R, Svátunkova J, Novotny J, Hejnova L, Ostadal B, Sedmera D. Heart rate changes mediate the embryotoxic effect of antiarrhythmic drugs in the chick embryo. *Am J Physiol Heart Circ Physiol*. 2013;304(6):H895-H902. doi:10.1152/ajpheart.00679.2012
59. Kasahara H, Ueyama T, Wakimoto H, et al. *Nkx2.5* homeoprotein regulates expression of gap junction protein connexin 43 and sarcomere organization in postnatal cardiomyocytes. *J Mol Cell Cardiol*. 2003;35(3):243-256. doi:10.1016/s0022-2828(03)00002-6
60. Kasahara H, Wakimoto H, Liu M, et al. Progressive atrioventricular conduction defects and heart failure in mice expressing a mutant *Csx/Nkx2.5* homeoprotein. *J Clin Invest*. 2001;108(2):189-201. doi:10.1172/JCI12694
61. Linhares VLF, Almeida NAS, Menezes DC, et al. Transcriptional regulation of the murine *Connexin40* promoter by cardiac factors *Nkx2-5*, *GATA4* and *Tbx5*. *Cardiovasc Res*. 2004;64(3):402-411. doi:10.1016/j.cardiores.2004.09.021
62. Biben C, Weber R, Kesteven S, et al. Cardiac septal and valvular dysmorphogenesis in mice heterozygous for mutations in the homeobox gene *Nkx2-5*. *Circ Res*. 2000;87(10):888-895.
63. Martinsen BJ. Reference guide to the stages of chick heart embryology. *Dev Dyn*. 2005;233(4):1217-1237. doi:10.1002/dvdy.20468
64. Metscher BD. MicroCT for developmental biology: a versatile tool for high-contrast 3D imaging at histological resolutions. *Dev Dyn*. 2009;238(3):632-640. doi:10.1002/dvdy.21857
65. Olejnickova V, Sedmera D. What is the optimal light source for optical mapping using voltage- and calcium-sensitive dyes? *Physiol Res*. 2020;69(4):599-607. doi:10.33549/physiolres.934471
66. Kolarova J, Novakova M, Ronzhina M, et al. *Isolated rabbit hearts-Databases of EGs and MAP signals. Computing in Cardiology Conference*, Zaragoza, Spain, 2013. IEEE; 2013:551-554. Accessed July 7, 2017 <http://ieeexplore.ieee.org/abstract/document/6713436/>
67. Vostarek F, Svátunkova J, Sedmera D. Acute temperature effects on function of the chick embryonic heart. *Acta Physiol*. 2016;217(4):276-286. doi:10.1111/apha.12691
68. Kolesova H, Capek M, Radochova B, Janacek J, Sedmera D. Comparison of different tissue clearing methods and 3D imaging techniques for visualization of GFP-expressing mouse embryos and embryonic hearts. *Histochem Cell Biol*. 2016;146(2):141-152.
69. Miller CE, Thompson RP, Bigelow MR, Gittinger G, Trusk TC, Sedmera D. Confocal imaging of the embryonic heart: how deep? *Microsc Microanal*. 2005;11(3):216-223. doi:10.1017/S1431927605050464

SUPPORTING INFORMATION

Additional supporting information can be found online in the Supporting Information section at the end of this article.

How to cite this article: Olejnickova V, Hamor PU, Janacek J, et al. Development of ventricular trabeculae affects electrical conduction in the early endothermic heart. *Developmental Dynamics*. 2022;1-13. doi:10.1002/dvdy.552